P-ISSN 1991-8941
E-ISSN 2706-6703
Vol. 20, No. 1 (2026)

Journal of University of Anbar for Pure Science
(JUAPS)

journal homepage: juaps.uoanbar.edu.iq

Open Access

Original Paper

Preparation and determining of a number of elemental complexes with hydrazone ligand derived from ibuprofen

Fayhaa.K Al-Jarah [1*], **Sahbaa A.Ahmed** [1]

[1]Department of Chemistry, College of Science, University of Mosul, Mosul, Iraq

ARTICLE INFO

Received: 30/05/2025
Accepted: 07/09/2025
Available online: 16/03/2026
April Issue
10.37652/juaps.2025.160913.1399

Cite @ JUAPS

Corresponding author
Fayhaa.K Al-Jarah
fayhaakamal60@gmail.com

ABSTRACT

This study addresses the synthesis and characterization of seven new complexes of a hydrazone ligand derived from a non-steroidal anti-inflammatory drug (ibuprofen) via condensation with p-nitroacetophenone, followed by reaction with cobalt(II), nickel(II), copper(II), zinc(II), and cadmium(II) chloride and nitrate salts. All complexes were prepared in a 1:2 metal-to-ligand molar ratio. The ligand and its complexes were characterized using FTIR, UV–Vis, 1H NMR, magnetic susceptibility measurements, molar conductivity, powder XRD, density functional theory (DFT), molecular docking, and bacteriological activity assays. Based on the physicochemical measurements and infrared spectral data, the ligand behaves as a neutral bidentate chelator, coordinating through the azomethine nitrogen and the amide oxygen. The combined evidence indicates the formation of hexa- and tetracoordinate complexes, consistent with octahedral, square-planar, or tetrahedral geometries. The research aims to prepare new ibuprofen-derived hydrazone complexes with potential applications in multiple fields. In pharmacological contexts, the prepared complexes may exhibit antimicrobial activity, as such compounds can interact with essential enzymes or disrupt bacterial cell walls. They may also show anti-inflammatory effects if part of the parent drug's activity is retained, potentially with improved efficacy or reduced side effects. In addition, hydrazone complexes containing metals such as cobalt(II) and copper(II) have been reported in multiple studies to interact with DNA or inhibit enzymes linked to cancer cell proliferation. Some complexes may also act as electron donors, enabling free radical scavenging and reducing oxidative stress associated with several diseases.

In coordination chemistry and analytical applications, these complexes can serve as models for understanding drug-metal interactions in vivo, supporting the design of new metallodrugs or improved drug absorption. Some complexes also exhibit fluorescence or visible spectral changes upon binding to specific molecules, enabling their use as sensors for ions or biomolecules. In organic chemistry, certain nickel- or copper-containing complexes can act as catalysts in oxidation and addition reactions.

Keywords: *Hydrazide, Ibuprofen, NSAIDs, P-nitro acetophenone*

1 INTRODUCTION

Hydrazides are important chemical compounds that contain the hydrazide group (–NH–NH_2), and they play significant roles in various chemical reactions. These compounds have been used in a wide range of industrial and pharmaceutical applications because of their unique chemical and biological properties, which have made them a focus of research in organic and biochemical chemistry [1]. Hydrazides can be synthesized by several methods, with one of the most common being the reaction of esters with aqueous hydrazine in ethanol. Hydrazides are also employed in various industrial applications, particularly as intermediates in the production of dyes and pesticides. In addition, these compounds have demon-

strated notable biological activity, making them valuable for developing new compounds with high efficiency and improved functionality [2]. Among the derivatives of hydrazides, hydrazone complexes are particularly important chemical compounds and have been widely used in industrial and research fields. These complexes are formed by the reaction of hydrazones with transition metals, yielding compounds with key properties, such as high stability and biological activity. Recent studies have shown that certain hydrazone-metal complexes can interact with cancer cells and inhibit their growth [3]. In the medical context, nonsteroidal anti-inflammatory drugs (NSAIDs) are widely used medications to relieve pain and inflammation. These drugs work by inhibiting cyclooxygenase (COX) enzymes, thereby reducing the production of prostaglandins, which are responsible for pain and inflammation. Ibuprofen, one of the most commonly used NSAIDs, is extensively prescribed to reduce inflammation and relieve pain [4]. It is used to treat several conditions, including headaches, joint pain, toothaches, and fever. Research has demonstrated that ibuprofen is effective in alleviating mild to moderate pain and has superior efficacy in some cases, such as dental pain or menstrual cramps [5].

2 EXPERIMENTAL

2.1 Preparation of an ester derived from ibuprofen (EP)

Ibuprofen structure is shown in Figure 1 [6]. The Ibuprofen ester, which naturally contains a carboxyl group, was prepared by dissolving 8.25 g of pure ibuprofen in 45 mL of ethanol and adding drops of concentrated sulfuric acid. The mixture was heated for about 16 h. After cooling, it was neutralized with a sodium bicarbonate solution. The ester separated as an oil layer and was extracted with ether. The ester was finally obtained as a colorless oil, with a boiling point of 107–110 °C [7].

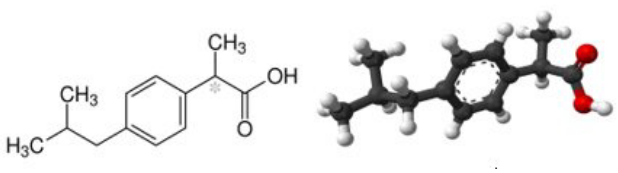

Fig. 1 Chemical composition of ibuprofen

2.2 Preparation of hydrazide derived from ibuprofen (HP)

The hydrazide was prepared by reacting 7.02 g of ester (EP), dissolved in 35 mL of ethanol, with 0.09 mol of aqueous hydrazine (23 mL). The mixture was heated for 30 h, after which the solvent was evaporated by concentration. It was then treated with ice water under stirring; the precipitate was separated and recrystallized from ethanol [8].

2.3 Preparation of hydrazones derived from ibuprofen hydrazide

Hydrazones were prepared by reacting equimolar amounts (1:1) of hydrazide (0.04 mol), dissolved in 50 mL of ethanol, with 0.04 mol of the carbonyl compound (p-nitroacetophenone), with the addition of a few drops of glacial acetic acid. After the addition was complete, the mixture was refluxed for 6 h. The solvent was evaporated, and the precipitate was collected, filtered, and washed with absolute ethanol. It was then recrystallized from ethanol.

2.4 Preparation of ligand complexes derived from ibuprofen

The complexes were prepared according to methods reported in the literature [9, 10]. The molar ratio was calculated as (1:2) (metal: ligand). A total of 0.002 mol of the salt MCl2·xH2O or M(NO3)2·xH2O was dissolved in 20 mL of absolute ethanol and added to a solution of ligand (0.008 mol) dissolved in 60 mL of hot absolute ethanol. The mixture was heated with continuous stirring for 3 h and then cooled. A precipitate formed, which was separated by filtration and washed with small amounts of ethanol [7, 8]. The reaction conditions, including solvent, temperature, and reaction time, are shown in Tables 1, 2, and 3. All preparation steps of the ligand are summarized in Figure 2.

2.5 Antibacterial activity

A bacterial suspension of the studied species was prepared in Nutrient Broth medium at a concentration of 1.5×10^8, standardized against a 0.5 McFarland standard tube in physiological buffered normal saline. A ligand suspension was prepared at a concentration of 3 mg/mL by dissolving the compounds in DMF (Dimethylformamide). Bacterial culture plates containing sterile Mueller–Hinton agar were prepared. After the medium solidified, wells were made in the agar using a cork borer to create holes

with a diameter of 6 mm. Using a sterile cotton swab, the surface of the nutrient agar was inoculated with the bacterial suspension prepared in step (1) for each of *Escherichia coli* (E. coli) and *Staphylococcus aureus* separately. This was done by dipping a sterile swab into each bacterial suspension, then spreading it over the agar surface in the wells. 50 µL of the ligand solution (3 mg/mL) was added to each well, while the solvent served as a control. The plates were incubated at 37 °C for 24 hours. The diameter of the inhibition zone around the wells was measured to assess the inhibitory effect of the tested compound on the growth of the bacteria studied. Samples of the antibiotics naproxen and ibuprofen were used as reference standards.

Table 1 Experimental Conditions for the Preparation of Ibuprofen Derived Compounds

Step	Compound	Solvent	Reactants / Catalysts	Conditions	Product Form
1	Ibuprofen Ester (EP)	Ethanol (45 mL)	Ibuprofen (8.25 g), few drops of conc. H_2SO_4	Reflux for 16 hours; then neutralized with $NaHCO_3$ and extracted with petroleum ether	Colorless oil (b.p. 107110°C)
2	Hydrazide (HP)	Ethanol (35 mL)	Ester (7.02 g), Aqueous hydrazine (23 mL, 0.09 mol)	Heated for 30 hours; solvent evaporated, then treated with ice water and recrystallized from ethanol	White crystalline solid
3	Hydrazone	Ethanol (50 mL)	Hydrazide (0.04 mol), Carbonyl compound (0.04 mol) , few drops glacial acetic acid	Reflux for 6 hours; solvent evaporated, product filtered, washed with absolute ethanol, and recrystallized	Crystalline solid
4	Metal Complex	Absolute ethanol (20 mL + 60 mL)	Metal salt (0.002 mol), Ligand (0.008 mol)	Heated with stirring for 3 hours; after cooling, precipitate filtered and washed with ethanol	Solid precipitate

Table 2 Chemical formulas of the prepared compounds and some of their properties

Symbol	Formula	The color	Melting point $\left(C^0\right)$	Yield percentage (%)
EP	$C_{15}H_{22}O_2$	White	-	88
HP	$C_{13}H_{20}N_2O$	White	76 – 78	82
L	$C_{21}H_{25}N_3O_3$	Orange	178 – 180	74

Table 3 Chemical formulas of the prepared complexes and some of their properties

Complex number	Chemical Formula	The color	Melting point (C^0)	Yield percentage (%)	Molar electrical conductivity ($cm^2.ohm^1.mol^{-1}$)
1	$[Co(L)_2Cl_2]$	Light Yellow	267-270	73	54.6
2	$[Co(L)_2(H2O)_2](NO_3)_2$	Brown	242-245	80	118.6
3	$[Ni(L)_2Cl_2]$	Light Yellow	255-258	84	43.5
4	$[Ni(L)_2(NO_3)_2]$	Golden brown	266-269	77	125.5
5	$[Cu(L)_2]Cl_2$	Yellow	256-259	70	38.2
6	$[Cd(L)_2]Cl_2$	Greenish Yellow	144-147	65	114.8
7	$[Zn(L)_2Cl_2]$	Yellow	>300	88	29.8

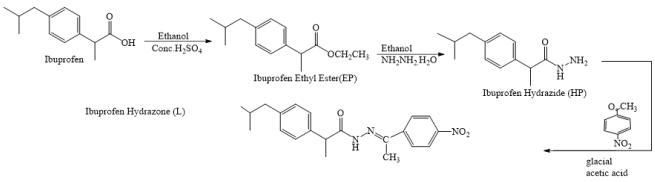

Fig. 2 Preparation steps of the ligand

3 RESULTS AND DISCUSSION

3.1 Molar electrical conductivity

The conductivity measurements were consistent with the proposed structural formulae of the prepared complexes. The prepared complexes (1, 3, and 7) were classified as neutral. In contrast, the generated complexes (2,4,5,6) were classified as electrolytes; their molar conductivity values indicate a (1:2) ratio. Table 3 lists the molar conductivity values of the generated complexes [11].

The proposed geometries of the new complexes are as follows: the Co(II), Ni(II), Cu(II), Zn(II), and Cd(II) complexes are octahedral, tetrahedral, and square planar. This assignment is supported by the magnetic property data and UV–Vis spectroscopy results, which are consistent with those reported in the literature. The results are summarized in Table 4.

Spectral data indicate that the hydrazone ligand coordinates with the metal ions through the azomethine nitrogen and the carbonyl (amide) oxygen atoms. In the Fourier-transform infrared (FT-IR) spectrum, the C=N stretching band shifts to lower frequencies compared with the free ligand, indicating involvement of the azomethine nitrogen in coordination. In addition, the decrease or disappearance of the C=O stretching band suggests coordination through the carbonyl oxygen. New bands appearing in the lower-frequency region (400–600 cm^{-1}) are often attributed to the formation of M–N and M–O bonds. Furthermore, the UV–Vis spectrum shows clear shifts in the position and intensity of the absorption bands upon complexation, reflecting alterations in the ligand's electronic environment upon metal binding. Collectively, these spectral changes provide strong evidence that the hydrazone ligand coordinates through both the azomethine nitrogen and the carbonyl oxygen.

3.2 FTIR

The infrared spectra of the ligand and the prepared complexes were recorded in the range of 400–4000 cm^{-1}, Figures 3 and 4. Table 5 shows the band values and their positions in the recorded spectra. The absorption bands

Table 4 The effective magnetic moment data and electronic spectral data of ligand and complexes

No.	compound	UV, Vis bands (cm^{-1})	Assignment	μ_{eff} B.M	Proposed Structure
L	$C_{21}H_{25}N_3O_3$	42275,39763	$\pi \rightarrow \pi^*$, n $\rightarrow \pi^*$	-	-
1	$[Co(L)_2Cl_2]$	(11325 – 13245 cm^{-1}) (14836 – 15685 cm^{-1}) (16766 – 22749 cm^{-1})	$^4T_1$ g(F) $\rightarrow$ $^4T_2$ g(F) (v_1) $^4T_1$ g(F) $\rightarrow$ $^4A_2$ g(F) (v_2) ^4T_1g(F) $\rightarrow$ ^4T_1g(P) (v_3)	4.66	Octahedral
2	$[Co(L)_2(H_2O)_2](NO_3)_2$	(11172 – 13467 cm^{-1}) (14718 – 16476 cm^{-1}) (18684 – 23522 cm^{-1})	$^4T_1$ g(F) $\rightarrow$ $^4T_2$ g(F) (v_1) $^4T_1$ g(F) $\rightarrow$ $^4A_2$ g(F) (v_2) ^4T_1g(F) $\rightarrow$ ^4T_1g(P) (v_3)	4.89	Octahedral
3	$[Ni(L)_2Cl_2]$	(12156 – 13624 cm^{-1}) (15265 – 18162 cm^{-1}) (22823 – 27395 cm^{-1})	$^3A_2$ g(F) $\rightarrow$ $^3T_2$ g(F) (v_1) $^3A_2$ g(F) $\rightarrow$ $^3T_1$ g(F) (v_2) $^3A_2$ g(F) $\rightarrow$ $^3T_1$ g(P) (v_3)	3.10	Octahedral
4	$[Ni(L)_2](NO_3)_2$	(11268 – 13083 cm^{-1})	^{3}T1(F) $\rightarrow$ $^3T_1$(P) (v_3)	3.71	Tetrahedral
5	$[Cu(L)_2]Cl_2$	16548	^{2}B1 g $\rightarrow$ ^{2}Eg $^2B_1$ g $\rightarrow$ $^2A_1$ g	1.84	Squreplanar
6	$[Cd(L)_2]Cl_2$	45725,39188	$\pi \rightarrow \pi^*$, n $\rightarrow \pi^*$	-	Tetrahedral
7	$[Zn(L)_2Cl_2]$	46547,38532	$\pi \rightarrow \pi^*$, n $\rightarrow \pi^*$	-	Octahedral

of the ligand were identified, and changes in the shape, intensity, and position of these bands upon coordination with metal ions to form complexes were examined. These spectral changes were then used to determine the coordination mode of the organic (hydrazone) ligand with the metal ions used in complex preparation [12–16].

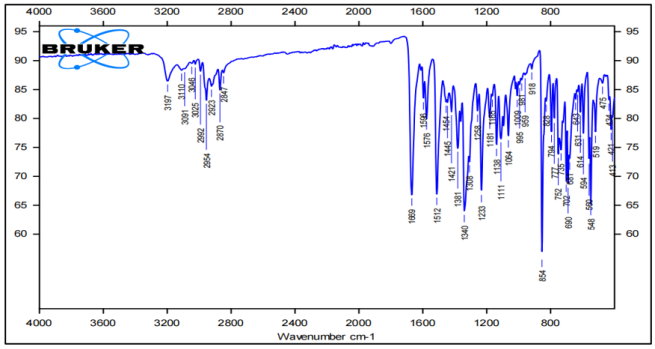

Fig. 3 FTIR of ligand

3.3 ^{1}H – NMR spectroscopy

Nuclear magnetic resonance (NMR) spectroscopy is used to study the nuclei of certain atoms, such as ^{13}C, ^{1}H, and ^{31}P. This technique employs radiofrequency (RF) waves, which are low-energy radiation with long wavelengths; their effect is observed through transitions between nuclear spin energy levels. All prepared ligands were examined by ^{1}H NMR spectroscopy. Tetramethylsilane (SiMe4) was used as the reference standard, and DMSO- d_6 was used as the solvent. The spectra were interpreted based on chemical shift values and integration [17].

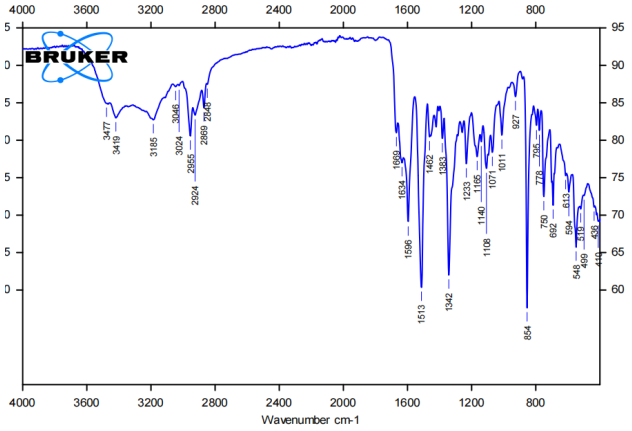

Fig. 4 FTIR of $[Co(L)_2Cl_2]$

Table 5 FTIR measurements of the prepared ligand and complexes

Formula chemical	ν (N-H)	ν (N-N)	ν (C = N)	ν (C = O)	ν (C-O)	ν (O-H)	δ (O – H)	ν (M-N)	ν (M-O)
L = $C_{21}H_{25}N_3O_3$	3046	1064	1596	1669	1233	3200-3300	1340	-	-
$[Co(L)_2Cl_2]$	3046	1011	1513	1596	1165	3200-3300	1342	499	613
$[Co(L)_2(H_2O)_2](NO_3)_2$	3042	1026	1576	1605	1220	3200-3300	1338	458	590
$[Ni(L)_2Cl_2]$	3048	1036	1570	1602	1235	3200-3300	1332	520	646
$[Ni(L)_2](NO_3)_2$	3046	1016	1565	1598	1222	3200-3300	1324	432	615
$[Cu(L)_2]Cl_2$	3040	1032	1556	1612	1218	3200-3300	1330	478	628
$[Cd(L)_2]_{Cl\,2}$	3046	1036	1552	1618	1225	3200-3300	1325	526	652
$[Zn(L)_2Cl_2]$	3042	1028	1578	1614	1234	3200-3300	1328	518	660

The ^{1}H NMR spectrum of the ligand (L) shows a doublet at 1.58 ppm assigned to the protons of two equivalent methyl groups (d, 3H, 2CH3) adjacent to the (−CH−) group. A doublet at 2.11 ppm is assigned to

a methyl group (d, 3H, −CH3) adjacent to the (−CH−) group. Two multiplet signals attributed to the (−CH−) protons appear at 2.94 and 3.53 ppm . A singlet at 3.08 ppm is assigned to the methyl protons (s, 3H, −CH3) adjacent to the (−C = N−) group, and a doublet at 3.38 ppm is assigned to the (CH2−) protons. In addition, aromatic protons appear as signals within the range 7.97 − 8.90ppm(m, 4H, Ar − H). A singlet at 11.43 ppm is assigned to the amide proton (s, 1H, −NH−) [18], Figure 5.

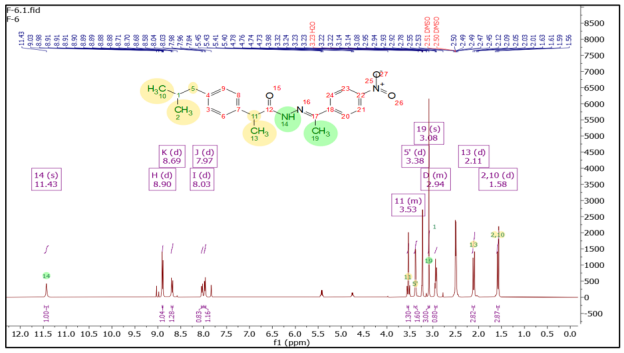

Fig. 5 The proton nuclear magnetic resonance of the ligand

3.4 Antibacterial activity

The bacteriological activity of the prepared ligands and some of their metal complexes was evaluated. This study included testing biological activity against laboratory-identified bacterial isolates using biochemical and microscopic methods. These bacteria are associated with many human diseases. The study included three human pathogenic bacteria: the Gram-positive *Staphylococcus aureus* and the Gram-negative bacteria *Escherichia coli*.

The method was based on preparing wells in the culture medium using a cork borer sterilized with absolute ethanol. The bacterial inoculum was then swabbed and spread evenly over the surface of Mueller–Hinton agar using sterile cotton swabs to ensure uniform distribution across the plate. The plates were left at 37 °C to allow absorption. Solutions of the prepared compounds were prepared at a concentration of 10 µg/mL in DMF, and 100 µL was added to each well. The plates were sealed with tape and incubated for 24 hours at 37 °C. The inhibition zone diameters were then measured using the method of Prescott (1996) with a ruler to determine the sensitivity of the tested compounds. Ciprodar was used as the antibiotic control. The prepared compounds showed very good effectiveness, as shown in Table 6 [19].

Table 6 Bacterial activity of ligand with complexes

No.	Tested compound	Bacteria	
		E.coli.(Graham negative)	*Staph. (Graham positive)*
L	$C_{21}H_{25}N_3O_3$	Zero	Zero
1	$[Co(L)_2Cl_2]$	30 mm	24 mm
2	$[Co(L)_2(H_2O)_2](NO_3)_2$	16 mm	17 mm
3	$[Ni(L)_2Cl_2]$	17 mm	23 mm
4	$[Ni(L)_2](NO_3)_2$	14 mm	Zero
5	$[Cu(L)_2]Cl_2$	30 mm	37 mm
6	$[Cd(L)_2]Cl_2$	37 mm	28 mm
7	$[Zn(L)_2Cl_2]$	16 mm	9 mm

The antibacterial activity of the above two bacterial strains was monitored in this study for each of the selected synthesized compounds and compared with the standard antibiotics ibuprofen and naproxen. As shown in Figure (6), the compound $[Cu(L)_2]Cl_2$ exhibited the highest inhibitory effect among the other compounds against *Staphylococcus aureus* bacteria. This activity may be attributed to the combined effect of the functional groups present in the compound, namely the hydroxyl, azomethine, methoxy, and amide carbonyl groups, which may have a direct or indirect effect on bacterial functions. Meanwhile, the compound $[Cd(L)_2]Cl_2$ also showed greater inhibitory ability, compared with the other compounds, against E. coli bacteria. This may be due to the presence of the alkyl functional group, which may contribute to antibacterial activity against the targeted strain. These results are consistent with those obtained by the researcher for other synthesized compounds containing the same functional group.

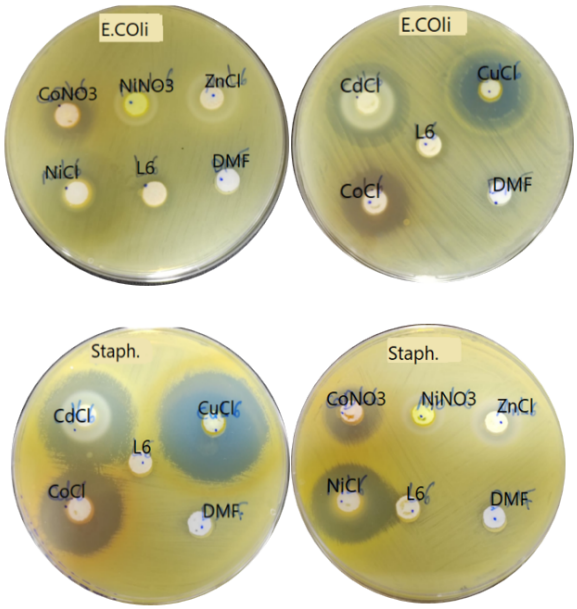

Fig. 6 Inhibition diameter of ligand and complexes

3.5 Molecular docking studies

Molecular docking was performed for the most effective compounds in inhibiting bacterial activity by targeting DNA gyrase, an enzyme involved in bacterial DNA replication. The study was conducted for two bacterial species, the Gram-negative *Escherichia coli* and the Gram-positive *Staphylococcus aureus*. The enzyme structures were obtained from the Protein Data Bank (RCSB PDB) for both species (ID: 1KZN and ID: 3G7B, respectively), as shown in Figure 7.

For docking of the ligand (L) with the DNA gyrase enzyme (ID: 1KZN) from coliform bacteria, the binding energy of the complex (enzyme + L) was (ΔG total binding energy = -6.8 kcal/mol), which was higher than that of the (enzyme + ibuprofen) complex (ΔG total binding energy = -5.5 kcal/mol). Key interactions included three hydrogen bonds involving VAL120, ALA96, and SER121. Additional interactions were observed with ASP45, ILE48, ILE194, ILE197, GLU42, and ILE165, which were associated with electrostatic and other noncovalent forces (van der Waals, π–alkyl, and C–H interactions, etc.) [20].

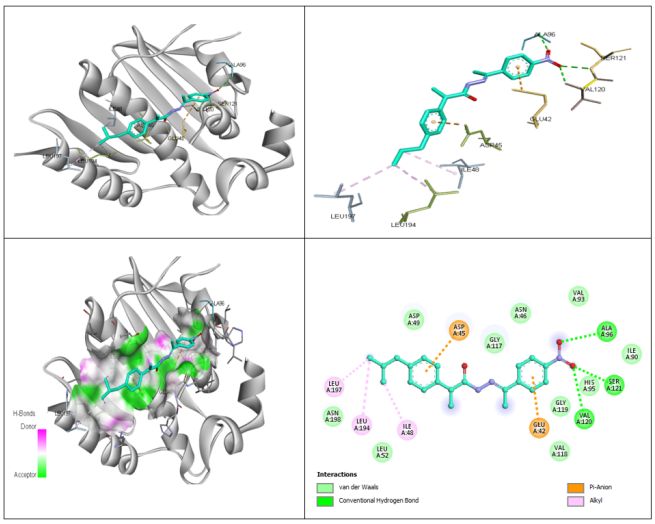

Fig. 7 The location of the ligand within the protein cavity ID 1KZN of coli bacteria in three D form, it shows the most important interactions between the functional groups in ligand and the amino acids ID 1KZN in a three D form, the location of the HB acceptor and donor that is formed between the amino acids and functional groups in L, it shows the most important interactions between the L functional groups and the type of amino acids ID 1KZN in a two dimensional form

After docking of the ligand (L) with DNA gyrase from *Staphylococcus aureus* (ID: 3G7B), the binding energy for the (enzyme + L) complex was (ΔG total binding energy = -7.3 kcal/mol), which was higher than that of the (enzyme + ibuprofen) complex (ΔG total binding energy = -6.9 kcal/mol). Key interactions between amino acid residues on the enzyme surface and the ligand included four hydrogen bonds involving LYS78, THR80, GLN66, and LYS170. Additional interactions were observed with THR141, VAL174, ILE148, HIS143, VAL165, ARG84, ASN54, ILE175, and ILE51, including π–alkyl, van der Waals, and $\pi - \pi$ stacking interactions, among other forces. Figure 8 shows the simulation results of (L) with *Staphylococcus aureus* DNA gyrase (ID: 3G7B) [21].

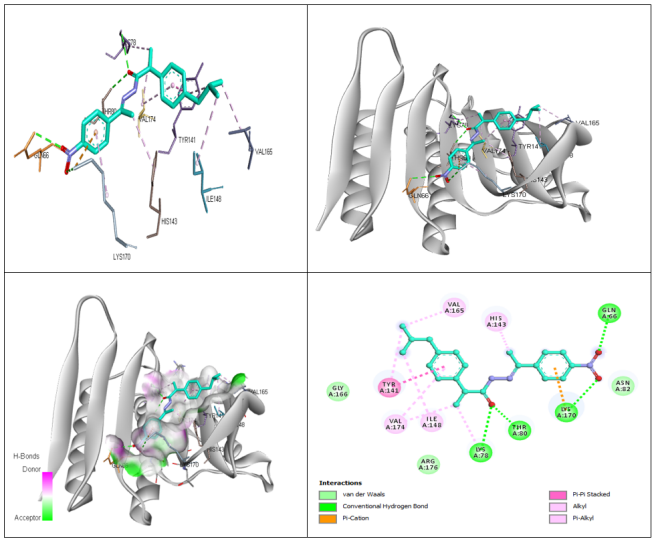

Fig. 8 The location of L within the protein cavity ID three g seven b of the staphylococcal bacteria in three D form, the interactions between the functional groups in ligand and the amino acids ID three g seven b in a three D format, HB acceptor and donor that is formed between the amino acids and functional groups in L, interactions between the ligand functional groups and the type of amino acids ID: three g seven b in a two dimensional form

3.6 Powder xrd studies

X-ray diffraction (XRD) is an analytical technique that provides information on the crystalline structure, chemical composition, and physical properties of materials and thin layers. This technique depends on monitoring the scattering intensity of an X-ray beam incident on the sample, as well as the angle of incidence, scattering, polarization, and wavelength. X-rays are electromagnetic radiation with photon energies and wavelengths in the range (0.1–100 Å) within the cosmic spectral series; in diffraction applications, only short-wavelength X-rays are

used. These powerful X-rays can penetrate deeply into materials and provide information about the structure of matter. The ligands and their complexes were examined using a device (Xrdx, Pert Phillips Holland). Data for these models were obtained and entered into a computer program prepared by a Dutch company called (X, perthigh score software package). Charts were obtained showing the relationship between intensity of absorption (intensity) and the measured diffraction data [22]. Analysis of the data obtained with (X, perthigh score software package) showed sharp diagnostic peaks in the charts, indicating the crystalline nature of the cobalt and nickel binary complexes; that is, the complexes have crystalline forms with crystalline planes and lattice structures. To interpret the results, Bragg's law [22] was used to calculate the spacing between crystalline planes (d-spacing), which represents the spacing between crystalline spaces. Tables 7 and 8 show the XRD data. In addition, the Debye–Scherer Raman and Jeyamurugan approach [22] was applied using the relationship ($D = K\lambda/\beta \times \cos(\theta)$) to calculate the crystallite size of complexes (1 and 3) for the metal ions Ni(II) and Co(II) coordinated with the ligand, Figures 9 and 11 show the Co(II) and Ni(II) complexes, Figures 10 and 12 show the X-ray diffraction (XRD) of Cobalt and Nickel complexes.

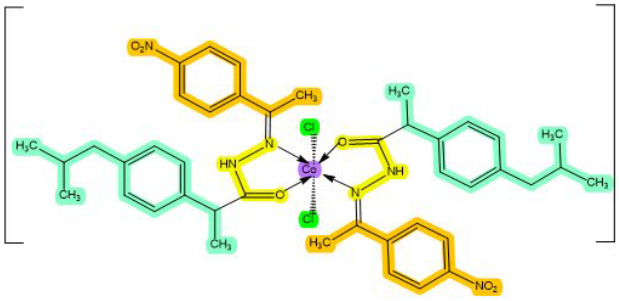

Fig. 9 Co(II) formed complex

3.7 Antioxidant activity

The antioxidant activity was determined using the DPPH free radical (2,2-diphenyl-1-trinitrophenylhydrazine). The ligand and its complexes were dissolved in a minimum volume of DMF and then further diluted with ethanol. These compounds donated hydrogen to reduce DPPH, producing a color change from dark purple to yellow. The DPPH radical-scavenging efficiency was evaluated by measuring absorbance at 517 nm, and the scavenging activity was calculated using the following equation:

$$\text{DPPH scavenging ability (\%)} = (\text{Abs.control} - \text{Abs.sample})/(\text{Abs.control}) \times 100$$

The first column below, titled "Ligand," represents the antioxidant activity of the ligand and its metal complexes. The ligand and the copper complex exhibited better antioxidant capacity than the other metal complexes at the higher concentrations tested. The RSA of the ligand and copper complex may be related to their hydrogen-donating ability [10]. Likewise, the high scavenging activity of the ligand may also contribute to its mild antimicrobial action; however, this interpretation should be supported by the antimicrobial data presented above [23].

Table 7 XRD data of the $[Co(L)_2Cl_2]$

Complex (1)	
Molecular Formula	$C_{42}H_{50}Cl_2CoN_6O_6$
Molecular weight	864.73 g/mol
Crystal system	Cubic
Space group	Fm-3m
Space group number:	225
Unit cell dimensions	a = 5.4650°A α = 90 (10°) b = 5.4650°A β = 90 (10°) c = 5.4650°A γ = 90 (10°)
Radiation	Cuα rotating anode
Calculated density (g/cm^)	5.42
Volume of cell (10^6pm^)	163.22
Z	2.00
Theta Range	45.6549 θ - 16.0121
Index ranges	$1 \le h \le 4$ $1 \le k \le 3$ $0 \le L \le 2$

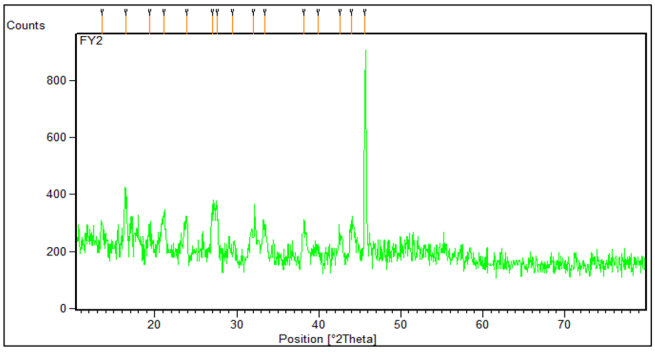

Fig. 10 XRD for $[Co(L)_2Cl_2]$

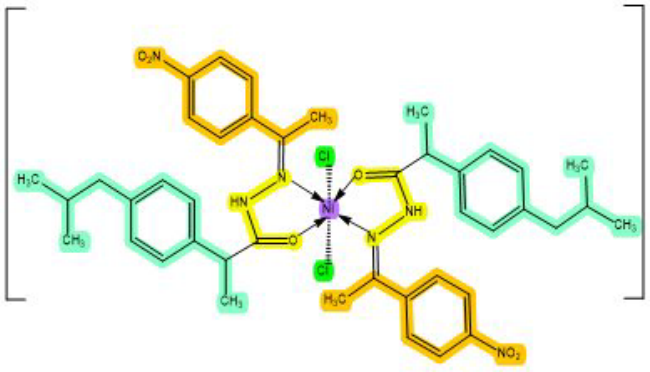

Fig. 11 Ni(II) formed complex

Table 8 XRD data of $[Ni(L)_2Cl_2]$

Complex (3)	
Molecular Formula	$C_{42}H_{50}Cl_2N_6NiO_6$
Molecular weight	864.49 g/mol
Crystal system	Rhombohedral
Space group	R-3
Space group number:	148
Unit cell dimensions	a = 5.0380°A α = 90 (10°) b = 5.0380°A β = 90 (10°) c = 13.7720°A γ = 120 (10°)
Radiation	Cuα rotating anode
Calculated density (g/cm^)	5.26
Volume of cell (10^6pm^)	302.72
Z	6.00
Theta Range	13.75-77.16 θ
Index ranges	$0 \le h \le 4$ $1 \le k \le 3$ $0 \le L \le 14$

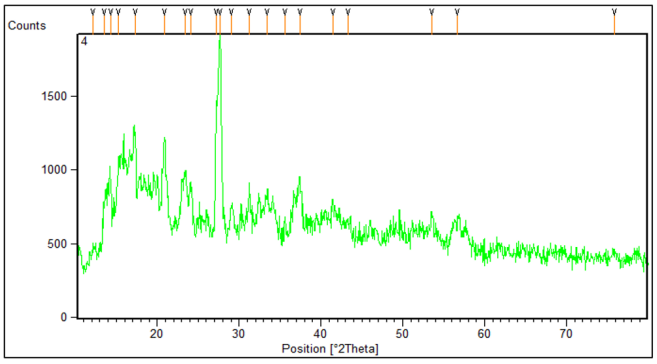

Fig. 12 XRD of $[Ni(L)_2Cl_2]$

Table 9 anti oxidant function of the ligand and complexes

Complex	Percentage scavenging activity of ligand and complexes		
	20μ g/ml	40μ g/ml	60μ g/ml
L = $C_{21}H_{25}N_3O_3$	78	76	82
$[Co(L)_2Cl_2]$	74	76	79
$[Ni(L)_2Cl_2]$	76	72	74
$[Cu(L)_2]Cl_2$	80	85	88
Ascorbic acid	84	86	92

3.8 Computational studies (dft)

The frontier orbitals, namely the highest occupied molecular orbital (HOMO) and the lowest unoccupied molecular orbital (LUMO), are among the most important orbitals in a molecule. The frontier-orbital energy gap (E_HOMO - E_LUMO) is a key parameter that provides information about the chemical reactivity and stability of a molecule and is also related to its electronic properties. A small energy gap (ΔE) is generally associated with higher chemical reactivity and lower stability, and such systems have been described as more reactive (soft) molecules [24].

The HOMO and LUMO energies of the ligand and its prepared complexes were calculated using density functional theory (DFT). These orbital energies were then used to calculate descriptors related to molecular stability and reactivity, including hardness (η), softness (σ), electronic chemical potential (μ), the global electrophilicity index (ω), and the excitation energy (eV). The stability order of the prepared complexes was discussed based on the global electrophilicity index (ω), where higher ω values indicate greater stability (Figure 13). Figure 14 indicates the suggested structures of the complexes.

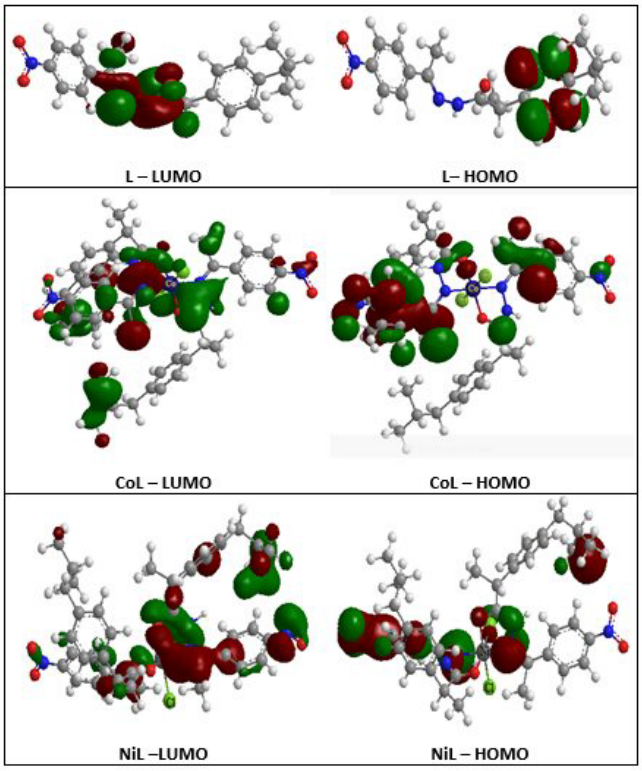

Fig. 13 HOMO and LUMO positions of the ligand and its prepared complexes

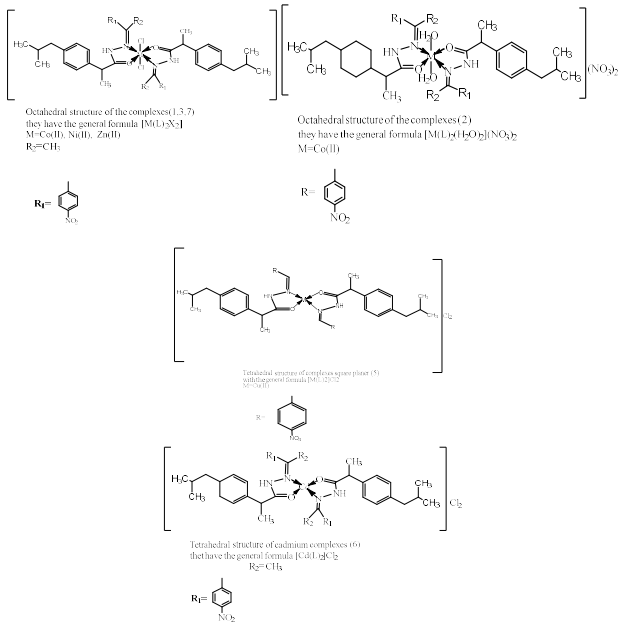

Fig. 14 suggested structures of the complexes

4 CONCLUSION

Chemical, physical, and spectroscopic analyses carried out in accordance with the above studies could indicate the structures of the complexes prepared by reacting the metals cobalt(II), nickel(II), copper(II), zinc(II), and cadmium(II) with their hydrazone ligands derived from some non-steroidal drugs (ibuprofen). All complexes were prepared in a metal:ligand molar ratio of (1:2), and the ligands were present as neutral bidentate species, thereby coordinating through the oxygen atom of the carbonyl group and the nitrogen atom of the azomethine group.

Acknowledgement

N/A

Author contributions

F.K. Al-Jarah designed the study and supervised the research. S.A. Ahmed conducted the experiments and performed data collection. Both authors contributed to data analysis and manuscript preparation. Both authors have read and approved the final version of the manuscript.

Funding source

No funds received.

Data availability

N/A

DECLARATIONS

Conflict of interest

The authors declare no competing interests.

Consent to publish

N/A

Ethical approval

N/A

REFERENCES

[1] Teixeira S, Castanheira EMS, Carvalho MA. Hydrazides as Powerful Tools in Medicinal Chemistry: Synthesis, Reactivity, and Biological Applications. Molecules. 2025;30(13):2852. 10.3390/molecules30132852

[2] Mali SN, Thorat BR, Gupta DR, Pandey A. Mini-Review of the Importance of Hydrazides and Their Derivatives—Synthesis and Biological Activity. In: The 2nd International Electronic Conference on Applied Sciences. ASEC 2021. MDPI; 2021. p. 21. 10.3390/asec2021-11157

[3] Ribeiro N, Correia I. A review of hydrazide-hydrazone metal complexes' antitumor potential. Frontiers in Chemical Biology. 2024;3. 10.3389/fchbi.2024.1398873

[4] Khalil NA, Ahmed EM, Tharwat T, Mahmoud Z. NSAIDs between past and present; a long journey towards an ideal COX-2 inhibitor lead. RSC Advances. 2024;14(42):30647–30661. 10.1039/d4ra04686b

[5] Lorenzi C, Cammarota I, Mazzetti V, Arcuri C, Carosi P, Pujia AM. The Use of Ibuprofen Arginate in Pain Management Following Third Molar Surgery—A Scoping Review. Applied Sciences. 2025;15(2):662. 10.3390/app15020662

[6] Jing Y, Zhao Q, Zhang J, Xue J, Liu J, Qin J, et al. RS, S (+)- and R ()-ibuprofen cocrystal polymorphs: Vibrational spectra, XRD measurement and DFT calculation studies. Heliyon. 2025;11(3):e41986. 10.1016/j.heliyon.2025.e41986

[7] Leonard J, Lygo B, Procter G. Advanced Practical Organic Chemistry. CRC Press; 2013. 10.1201/b13708

[8] Han MI, Atalay P, Tunc CU, Unal G, Dayan S, Aydın O, et al. Design and synthesis of novel (S)-Naproxen hydrazide-hydrazones as potent VEGFR-2 inhibitors and their evaluation in vitro/in vivo breast cancer models. Bioorganic & Medicinal Chemistry. 2021;37:116097. 10.1016/j.bmc.2021.116097

[9] Muley A, Kumbhakar S, Raut R, Mathur S, Roy I, Saini T, et al. Mononuclear copper(<scp>ii</scp>) complexes with polypyridyl ligands: synthesis, characterization, DNA interactions/cleavages and in vitro cytotoxicity towards human cancer cells. Dalton Transactions. 2024;53(28):11697–11712. 10.1039/d4dt00984c

[10] Ammal P R, Prasad AR, Joseph A. Synthesis, characterization, in silico, and in vitro biological screening of coordination compounds with 1,2,4-triazine based biocompatible ligands and selected 3d-metal ions. Heliyon. 2020;6(10):e05144. 10.1016/j.heliyon.2020.e05144

[11] Naseri Boroujeni S, Maribo-Mogensen B, Liang X, Kontogeorgis GM. Theoretical and practical investigation of ion–ion association in electrolyte solutions. The Journal of Chemical Physics. 2024;160(15). 10.1063/5.0198308

[12] Kondaiah S, Reddy GNR, Kumar BV, Chowdary PG, Reddy BR. Synthesis, characterization and biological activity of a novel p-toulic hydrazone and resacetophenone schiff base (RAPPTH) ligand and their metal complexes. J Der Pharma Chemica. 2015;7(10)

[13] Sharma VK, Srivastava S, Srivastava A. Spectroscopic, Thermal and Biological Studies on Some Trivalent Ruthenium and Rhodium NS Chelating Thiosemicarbazone Complexes. Bioinorganic Chemistry and Applications. 2007;2007:1–10. 10.1155/2007/68374

[14] Roy S, Mal S, Banik R, Das S, Dlhan L, Titis J, et al. Two isostructural complexes of Ni(<scp>ii</scp>) and Zn(<scp>ii</scp>) with violurate and pyridine: a detailed structural, theoretical, magnetic, and NMR investigation. CrystEngComm. 2023;25(46):6503–6511. 10.1039/d3ce00871a

[15] Singh S, Yadav HS, Yadava AK, Rao DP. Synthesis of Oxovanadium(IV) Complexes with Tetraaza Coordinating Ligands. Journal of Chemistry. 2012;2013(1). 10.1155/2013/947325

[16] Nakamoto K. Infrared and Raman Spectra of Inorganic and Coordination Compounds: Part B: Applications in Coordination, Organometallic, and Bioinorganic Chemistry. Wiley; 2008. 10.1002/9780470405888

[17] Patorski P, Wyrzykiewicz E, Bartkowiak G. Synthesis and Conformational Assignment of N-(E)-Stilbenyloxymethylenecarbonyl-Substituted Hydrazones of Acetone ando-(m- andp-) Chloro- (nitro-) benzaldehydes by Means of and NMR Spectroscopy. Journal of Spectroscopy. 2013;2013:1–12. 10.1155/2013/197475

[18] Birgül K, Yıldırım Y, Karasulu HY, Karasulu E, Uba AI, Yelekçi K, et al. Synthesis, molecular modeling, in vivo study and anticancer activity against prostate cancer of (+) (S)-naproxen derivatives. European Journal of Medicinal Chemistry. 2020;208:112841. 10.1016/j.ejmech.2020.112841

[19] Norouzbahari M, Salarinejad S, Güran M, Şanlıtürk G, Emamgholipour Z, Bijanzadeh HR, et al. Design, synthesis, molecular docking study,

and antibacterial evaluation of some new fluoroquinolone analogues bearing a quinazolinone moiety. DARU Journal of Pharmaceutical Sciences. 2020;28(2):661–672. 10.1007/s40199-020-00373-6

[20] Al-Wabli RI, Alsulami MA, Bukhari SI, Moubayed NMS, Al-Mutairi MS, Attia MI. Design, Synthesis, and Antimicrobial Activity of Certain New Indole-1,2,4 Triazole Conjugates. Molecules. 2021;26(8):2292. 10.3390/molecules26082292

[21] Al-burgus AF, Ali OT, Al-abbasy OY. New spiro-heterocyclic coumarin derivatives as antibacterial agents: design, synthesis and molecular docking. Chimica Techno Acta. 2024;11(3). 10.15826/chimtech.2024.11.3.08

[22] El-Shaer A, Ezzat S, Habib MA, Alduaij OK, Meaz TM, El-Attar SA. Influence of Deposition Time on Structural, Morphological, and Optical Properties of CdS Thin Films Grown by Low-Cost Chemical Bath Deposition. Crystals. 2023;13(5):788. 10.3390/cryst13050788

[23] Singh A, Gogoi HP, Barman P, Guha AK. Novel thioether Schiff base transition metal complexes: Design, synthesis, characterization, molecular docking, computational, biological and catalytic studies. Applied Organometallic Chemistry. 2022;36(6). 10.1002/aoc.6673

[24] Waziri I, Wahab OO, Mala GA, Ismaila MB, Umaru U, Abd El-Maksoud MS, et al. Synthesis, Characterization, Biological Evaluation, DFT Calculations, and Molecular Docking Study of Transition Metal Complexes Derived From a Schiff Base Ligand. Chemistry & Biodiversity. 2025;22(11). 10.1002/cbdv.202500940

How to cite this article

Al-Jarah FK, Ahmed SA. Preparation and determining of a number of elemental complexes with hydrazone ligand derived from ibuprofen. Journal of University of Anbar for Pure Science. 2026; 20(1):190-200. doi:10.37652/juaps.2025.160913.1399